Study on the new topology of Power Electronic Transformer

ZHIBING WANG[1], KUSHAN YU[2], XIAOXIN ZHOU[2]
1 School of Electric Information and Electrical Engineering
Shanghai Jiaotong University
2 China Energy Power Research Institute
Xiaoying East Road, District Haidian, Beijing
CHINA
wangzhibing@sjtu.edu.cn

Abstract: - This paper presents a mixed topology of Power Electronic Transformer based on Three-Level converter and H-Bridges. It does take into account two conditions, which includes the development of power electronic devices and manufacturing level of high-frequency transformer in the future. First the paper introduced the fundamentals of PET, and then studied on the mathematical model of the new topology in detail. In order to verify the validity of the new topology, the model of Power Electronic Transformer was simulated by MATLAB/PST toolbox, and indicated the inherent problem, which is unbalance of the neutral point voltage. Therefore, the paper proposed control strategies to maintain the balance, and suppress the effect of ripple voltage on common DC bus. Eventually simulations and experimental results validate the feasibility of the new topology and control strategies.

Key-Words: - Distributed Generations (DGs), Intelligent Universal Transformer (IUT), Power Electronic Transformer (PET), Solid State Transformer (SST), Space Vector Modulation (SVM), Power Factor Correction (PFC), Renewable Energy Source (RES), Smart Grid (SG)

1 Introduction

Now with the development of Smart Grid, power system requires an increasing penetration of the renewable energy source or other distributed generations near load center, which will be a low-cost electricity from the perspective of customers, but now the connecting technology of RES is not perfect, which must be developed in some aspects of connecting devices, for instance in topology, and in control strategy aspects, and so forth. With the intermittent and volatility of RES or DGs, the connecting devices seriously affected the security of power system, especially power quality. Because of that, some researchers carried out the related technologies around the world.

In the era of Smart Grid, customers have advanced requirements for power supply, such as various custom power qualities, kinds of power sources, and so on. Traditional transformer can't satisfy the demands of SG in medium-low voltage distribution network.

In addition, users hoped that the transformers could supply a kind of functions, such as power factor correction, voltage regulation, voltage sag and swell elimination, voltage flicker reduction and protection capability in fault, even the connection of RES. In a similar way, the transformer was required to provide the cascade power quality and various types of power sources for industrial consumers.

Power Electronic Transformer is a better solution, which can meet the demands of customers. In 1997, paper [1] is to realize an electronic transformer as a power delivery component in electric distribution system, which has a study in several aspects, including electronic transformer topologies, mathematical analysis, and experimental results etc. It used high frequency modulated AC/AC transformer, this design has the benefit of reducing the size and weight, and the electrical stress factors is more reasonable, but the function of topology is limited, the harmonic can flow bi-direction, and the level of bi-directional switch is poor interiorly.

Reference [2][16] proposed an optimum design of PET, in the design process, the PFC and DC/DC converters had been integrated to achieve higher efficiency, and the design can achieve typical functions of SG and other benefits. At the same time, it may be possible to commercialize nearly, but the series or parallel connection of converters had been used, the reliability of PET gravely depended on voltage level and the type of semiconductor switch.

Reference [3][5] programmed the applications of PET in Smart &Strong Grid in China, paper [4] supposed a new multilevel topology of IUT, considering the development of semiconductor in the future, ABB company supplied a solution of

PET in reference [6], in which the company provided a cascade H-Bridge topology, and gave some experimental results, but the structure required more switches.

This paper presents a new topology of PET, which is based on the development of power electronic devices in the future. There were fewer switches for three level converter structures, which would improve the reliability of PET. Equivalently, the topology is insensitive to the harmonics, promotes power quality, eliminates the effects of the connecting on RES or DGs, and provides a kind of power sources. However, some faults existed in this PET, but the paper gave a perfect solution, both simulations and experimental results verified the feasibility of the new topology.

The paper is organized as follows.

2 Proposed Topology

From 2009, Smart Grid has been researched in the world, especially in China, the distribution system becomes an active network, the requirement of PET is more and more, many researchers had published their production in magazines. Some investigations such as topology, control strategy, and reliability, are provided in paper [6][7][8]. But these new proposals were based on the ideal conditions, not considering the engineering factors. Therefore, a site-based practicable PET is desirable. This paper proposed a new topology of such a PET. Figure 1(a) showed the sketch structure, which is based on the Turn-Off Device, and the structure of output stage was decided by the requirement of power supply. As a comparison, the typical structure of existing PET is also shown in figure 1(b).

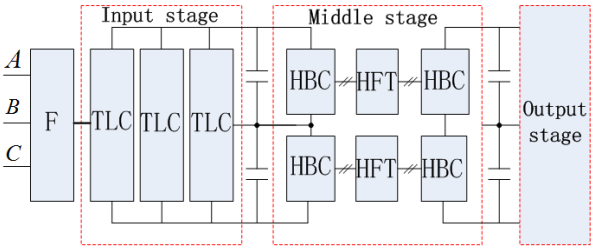

(a) A new topology structure of PET

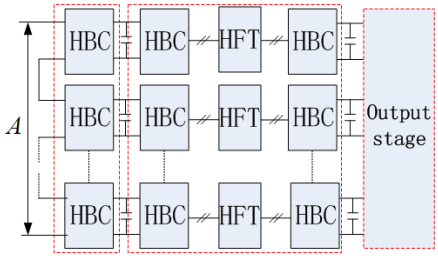

(b) The typical structure of single PET

Fig.1 The structure of PET

As shown in Fig.2, the model F in Fig.1 is a LCC three-order filter, which is composed of L, C R components. The capability of LCR filter, which restraints the high frequency interference, is better than LC filter, and it can reduce the gain in resonance peak point.

In fact due to the powerful performance, the structure of filter will be widely used to medium voltage converter in smart distribution network.

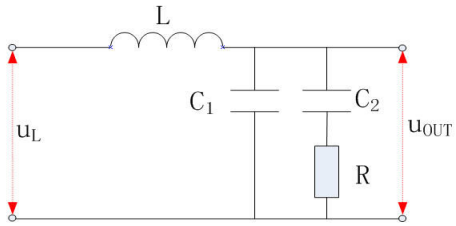

Fig.2 The structure of input or output filter

The TLC topology is shown in figure 3. In future, due to the development of S_iC switches, even the model will be composed of two levels converter, the switch frequency will be improved, and the size of PET will be reduced largely.

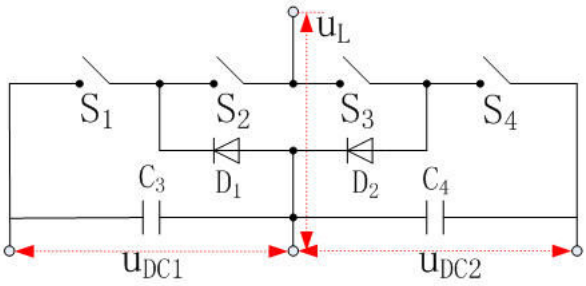

Fig.3 The structure of TLC

Figure 4 displayed the HBC model, which is based on the Turn-Off device. In the future the switch will be produced by S_iC.

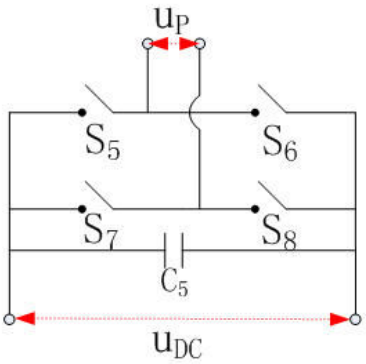

Fig.4 The structure of HBC

Compared with traditional transformer, the PET have some advantages, for example, regardless of what input voltage is, with the suitable control, the output voltage could maintain to be sinusoidal, and contain fewer harmonics. At the same time, the active power and reactive power can be controlled freely.

Owing to the DC bus, the harmonics can't interpenetrate each stage, commonly it is used to prevent secondary faults from propagating through the transformer.

In addition, as a result of the limiter of power in high frequency transformer now , the middle stage must use plenty of H-Bridges and high-frequency transformers, which will divide DC-bus into some grates, the topology of PET is more practical.

Additionally, it is necessary for PET topology to consider the development of semiconductor, core material, and engineering conditions; the structure will be modular, compacted, standard, and intelligent in the future.

However the topology is also with some disadvantages, such as the voltage of neutral point of TLC DC-Bus is not balanced normally. The next chapters will establish mathematical model of the mixed PET in detail, discuss the cause why the neutral potential were imbalanced, and design the solution for the common point particularly.

3 Mathematical Model Analysis

As shown in figure 1, the structure of PET consists of input stage, middle stage, output stage , and input/output filter. The structure of input filter is in common with output stage, and the section will discuss the mathematical model with each part.

3.1 Analysis of LCC Filter

In order to eliminating the effects of harmonics, it is necessary to add a filter. As shown in Figure 2, the open-loop transfer function of LCC filter is

$$G(s)=\frac{u_{OUT}(s)}{u_L(s)}=\frac{sRC_2+1}{s^3RC_1C_2L+S^2(C_1+C_2)L+SRC_2+1} \quad (1)$$

Generally, C_2 equals to 1/3 or 1/2 (C_1+C_2). Assuming

$$C_1=C_2=C \quad (2)$$

The transfer function will be simplified as follows:

$$G(s)=\frac{u_{OUT}(s)}{u_L(s)}=\frac{sRC+1}{s^3RC^2L+2S^2CL+SRC+1} \quad (3)$$

From equation (3), the Natural Oscillation Frequency is

$$\omega_n=\frac{1}{\sqrt{LC}} \quad (4)$$

The Damping Ratio is

$$\xi=\frac{1}{R}\sqrt{\frac{L}{C}} \quad (5)$$

Equation (5) implied that, the Damping Ratio has relationship with the damping resistor. If the component L and C are fixed, the more the value of resistor is, the smaller the Damping Ratio is.

Both Bode diagrams of LC filter and this LCC filter are shown in figure 5. Compared to the LC filter, the capability of restraining high frequency jamming of LCC filter is the same. Due to increasing a pole in the Natural Oscillation Frequency, the gain of resonance peak becomes smaller, and then the stability of system will be improved. In other word, the damping coefficient of system is greater.

Since damping resistor is an energy-consuming component, it will reduce the efficiency of PET. Therefore, it is important for the choice of damping resistor.

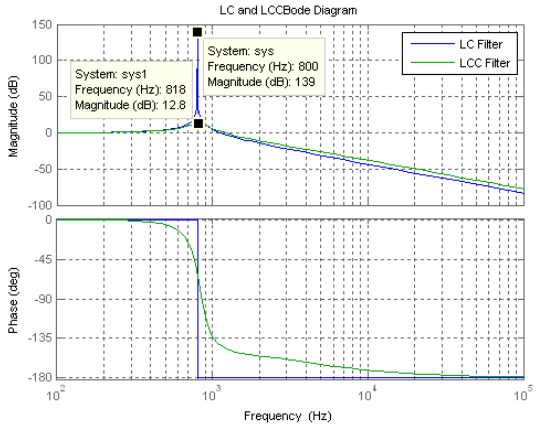

Fig.5 The Bode diagram of LC and LCC filter

3.2 Analysis of Input Stage

The topology of input stage is shown in figure 3, and so is for output stage. This is TLC structure, and has been utilized widely. References [9][10][11] proposed some methods of Space Vector Modulation, which also can be applied to the multilevel converter above three-level converter, and can effectively disperse the switching noise energy into a wide frequency range. Papers [12][13] provided the applications of three level converter in the field of renewable energy sources.

Generally speaking, the topology was used in the location of medium voltage and high power as a result of high efficiency. With the development of SG, this kind of converter will be widespread in power system.

This paper presents a new topology of PET, which is based on TLC. By analyzing the structure of input stage, due to the symmetry between three phases, the switch table of single phase TLC is shown in table 1.

Table 1 the switch table of TLC

S_x	S_y	Sign(I_x)	U_L
1	1	+/-	U_{dc}/U_{dc}
1	0	+/-	$-U_{dc}/U_{dc}$
0	1	+/-	0/0
0	0	+/-	$-U_{dc}/-U_{dc}$

Where S_x and S_y are the switch functions and stands for the S_1,S_3 or S_2,S_4 switch state separately. U_{dc} is the voltage of divided capacitors, sign(I_x) shows the direction of inductive current.

When $U_L=U_{dc}$ and sign(I_x)<0, the switch state can be two choices: $S_x=S_y=1$,and $S_x=1$,$S_y=0$, at the same time, when $U_L=-U_{dc}$ and sign(I_x)>0, the switch state can be also two choices: $S_x=S_y=0$,and $S_x=0$,$S_y=1$,.Therefore, the switch state is redundancy state.

The voltage of DC bus equals to $2U_{dc}$, and the DC bus has been divided into U_{dc1} U_{dc2}, U_{dc1} doesn't always equal to U_{dc2}, but fluctuate in line with frequency tripling. If out of control, the voltage of neutral point of three level converters will be drifted, the harmonic level of output voltage becomes ample. Therefore, the key point of TLC is to maintain the steady state of neutral point voltage.

3.3 Analysis of Middle Stage

The unit of middle stage is shown in figure 6, which is composed of H-Bridges, the power flow can bi-directionally run by adjusted control strategies, and the primary or secondary power were isolated by high frequency transformer.

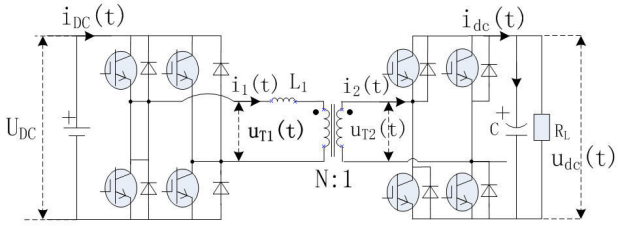

Fig.6 The structure of middle stage

By analyzing the structure of middle stage, the transient mathematical model is that

$$\begin{cases} L_1 \dfrac{di_{DC}}{dt} = d_{eff} * u_{DC} - S_i * N * u_{dc} \\ C \dfrac{du_{dc}}{dt} = \dfrac{N * i_{DC}}{d_{eff}} - \dfrac{u_{dc}}{R_L} \end{cases} \tag{6}$$

Where S_i is a switch function; N is the turn ratio of high frequency transformer; d_{eff} is the valid duty cycle of switch.

If middle stage is in steady state operation, in other word, the inductor and capacitor do not exchange energy. Equation (6) will be

$$\begin{cases} 0 = d_{eff} * u_{DC} - S_i * N * u_{dc} \\ 0 = \dfrac{N * i_{DC}}{d_{eff}} - \dfrac{u_{dc}}{R_L} \end{cases} \tag{7}$$

The steady state mathematical model is as follows

$$\begin{cases} I_{DC} = \dfrac{D}{N} I_L \\ U_{DC} = \dfrac{N * U_{dc}}{D} \end{cases} \tag{8}$$

Therefore, large-signal average mathematical model is shown as figure 7.

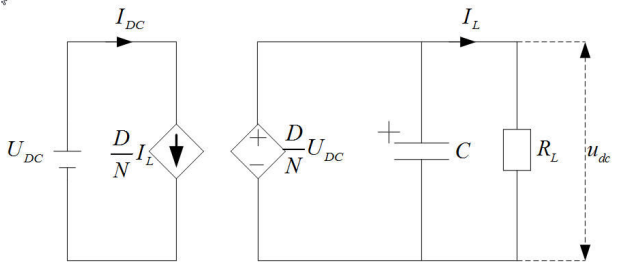

Fig.7 Large signal average mathematical model of middle stage

Having an assumption, all parameters consist of a steady state and a transient component. If parameters are

$$\begin{cases} i_{DC} = I_{DC} + \hat{i}_{DC} \\ u_{DC} = U_{DC} + \hat{u}_{DC} \\ d_{eff} = D_{eff} + \hat{d}_{eff} \\ u_{dc} = U_{dc} + \hat{u}_{dc} \end{cases} \tag{9}$$

Assumption the two order quadratic equation is small enough; the model will be described as follows.

$$\begin{cases} L_1 \dfrac{d\hat{i}_{DC}}{dt} = D_{eff} \hat{u}_{DC} + U_{DC} \hat{d}_{eff} - S_i * N * \hat{u}_{dc} \\ C \dfrac{d\hat{u}_{dc}}{dt} = \dfrac{N * \hat{i}_{DC}}{D_{eff}} - \dfrac{\hat{u}_{dc}}{R_L} \end{cases} \tag{10}$$

The small-signal mathematical model is deduced as figure 8.

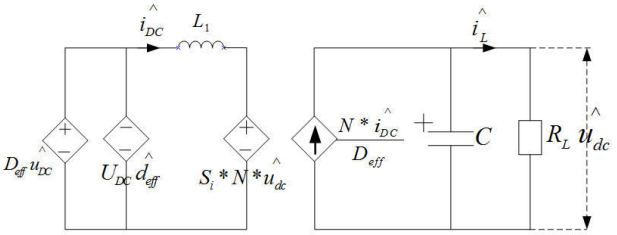

Fig.8 Small signal mathematical model of middle stage

From equation (10) and figure 8, the open-loop transfer function is as below.

$$G_{\hat{u}_{dc}\hat{d}_{eff}}(s)=\frac{U_{DC}*N*R_L}{D_{eff}*L_1*C*R_LS^2+L_1*D_{eff}*S+S_i*N^2*R_L} \quad (11)$$

$$G_{\hat{u}_{dc}\hat{u}_{DC}}(s)=\frac{D_{eff}*N*R_L}{D_{eff}*L_1*C*R_LS^2+L_1*D_{eff}*S+S_i*N^2*R_L} \quad (12)$$

$$G_{\hat{u}_{dc}\hat{i}_{DC}}(s)=\frac{NR_L}{D_{eff}*(R_LCs+1)} \quad (13)$$

From equation (11)(12)(13), there existed two-order transfer function between output voltage of middle stage and duty cycle, and there is a relationship between leakage inductance and damping ratio; there existed two-order transfer function between output voltage of middle stage and input voltage yet, by analyzing the functions, the control of input voltage or duty cycle is equivalent.

To synthesize above equations, the implementation diagram in detail is clarified as figure 9. If taking into account the bi-directional flow, it is necessary for special control strategies, but the transfer function is equally applicable. Due to the separation of middle stage, the transfer power of each modular is disproportion. Accordingly, the voltage of neutral point will be imbalance.

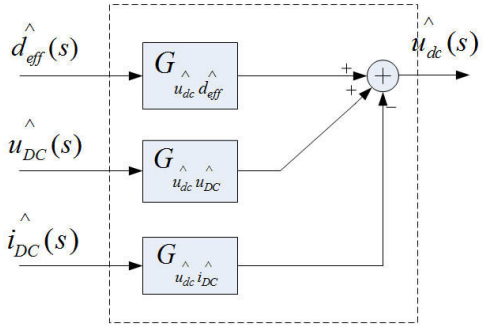

Fig.9 The implementation diagram of mathematical model for middle stage

In conclusion, the mathematical model of PET is complicated, which is a high-order system, if considering the stray parameters, the open-loop transfer function of PET is more than eight-order. Wherefore the section has the detail model for each stage, at one time, the section also proposes the key points of hardware design, and the next portion will provide the control strategies about some segments.

4 Control Strategies

The balance of neutral point clamped voltage is important for the performance of PET. This section introduced the cause of imbalance, and supplied the control strategies.

4.1 The Cause of Imbalance

There are two aspects for the unbalance, one of which is the inner factors of TLC; another is the disequilibrium of supply power in middle stage.

4.1.1 The Inner Factor

In order to understand the clear reasons for the imbalance, assuming power energy flow in each H-Bridge is balanced. Figure 10 rendered the equivalent schematic diagram of Three-Level Converter.

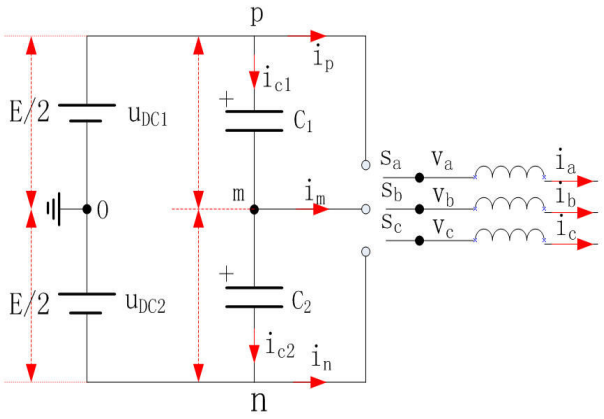

Fig.10 The equivalent schematic of output stage

Assuming the voltage of DC-Bus is steady state, according to the relationship between i_p, i_m, i_n, and i_a, i_b, i_c, there is the following mathematical expressing.

$$\begin{bmatrix}v_{ao}\\v_{bo}\\v_{co}\end{bmatrix}=\begin{bmatrix}S_{ap}&S_{am}&S_{an}\\S_{bp}&S_{bm}&S_{bn}\\S_{cp}&S_{cm}&S_{cn}\end{bmatrix}\begin{bmatrix}v_{po}\\v_{mo}\\v_{no}\end{bmatrix}=S\begin{bmatrix}v_{po}\\v_{mo}\\v_{no}\end{bmatrix}=S\begin{bmatrix}E/2\\v_{mo}\\-E/2\end{bmatrix} \quad (14)$$

$$\begin{bmatrix}i_p\\i_m\\i_n\end{bmatrix}=\begin{bmatrix}S_{ap}&S_{bp}&S_{cp}\\S_{am}&S_{bm}&S_{cm}\\S_{an}&S_{bn}&S_{cn}\end{bmatrix}\begin{bmatrix}i_a\\i_b\\i_c\end{bmatrix}=S^T\begin{bmatrix}i_a\\i_b\\i_c\end{bmatrix} \quad (15)$$

Where

$$S_{ij}=\begin{cases}1 & \text{node i connects node } j\\0 & \text{node i doesn't connect node } j\end{cases}, \text{ and } \begin{cases}i\in(a,b,c)\\j\in(p,m,n)\end{cases} \quad (16)$$

$$\sum_{j\in(p,m,n)}S_{ij}=1 \quad i\in(a,b,c) \quad (17)$$

Considering the principle of Voltage-Second Balance, when it is in the transient process for the system, the following mathematical expression is established.

$$i_{c1}=C_1\frac{dv_{pm}}{dt}=C_2\frac{d(-v_{mn})}{dt}=-i_{c2}=\frac{1}{2}i_m \quad (18)$$

Assuming the voltage of DC-bus is constant, there will be

$$C_1\frac{dv_{mo}}{dt}=C_1\frac{dv_{mp}}{dt}+C_1\frac{dv_{po}}{dt}=-C_1\frac{dv_{pm}}{dt}=-\frac{1}{2}i_m \quad (19)$$

From equation (18) and (19), the variation tendency of v_{mo} is the same with the v_{mn}, then combining the equation (15) and (19) can be substituted that.

$$C_1\frac{dv_{mo}}{dt}=-\frac{1}{2}(S_{am}i_a+S_{bm}i_b+S_{cm}i_c)$$
$$=-\frac{1}{2}[(S_{am}-S_{cm})i_a+(S_{bm}-S_{cm})i_b] \quad (20)$$

The voltage of neutral point is not only related with the phase current, but also existed relationship with the switching states as shown in equation (20). Due to the coupled-relation between i_a i_b and i_c in three-phase three-wire power system, we can maintain the balance of capacitor voltage by only control phase current i_a and i_b.

4.1.2 The Unbalanced Power of H-Bridges

The DC-bus of input stage has been divided into two components, by capacitor, and control strategies of each H-bridge are independent. Accordingly the power of modular is different from each other. The imbalanced power of middle voltage affected neutral point voltage. Figure 11 provided the equivalent schematic diagram of the middle stage.

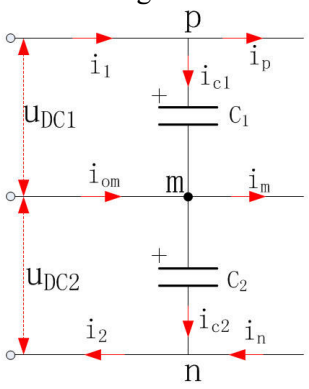

Fig.11 The equivalent schematic of middle stage

Assuming the load is constant, the average of i_p or i_n is fixed, by analyzing the structure of equivalent model, we see that

$$\begin{cases} C_1 du_{pm}/dt = i_1 - i_p = i_{C1} \\ C_2 du_{mn}/dt = i_{on} - i_m = i_{C2} \\ i_{om} = i_1 - i_2 \\ i_m = i_p - i_n \end{cases} \quad (21)$$

From equation (21), and combining equations (11) (12) and (13) above, the power of middle stage is connected with U_{DC} D_{eff} and I_{DC}. If the average power of middle unit is not equal in switch period, the voltage will be fluctuated with the current, and there is the one-order function between the capacitor voltage and current of DC-Bus branch, the result is in accordance with equations (11) (12) (13). Therefore, in order to control the balance of neutral point, the critical point is to control the current of neutral point, which is inflow or outflow.

4.2 Analysis of Control Strategies

Researchers have developed the strategies for many years. Reference [14] proposed a new method for the neutral point potential variation, but the direction of phase current doesn't take into account, the purpose of control is limited, even the control strategy depraves the neutral point potential, and the input current wave will be distortion. At the same time, some paper supplied a kind of methods, which is composed of half bridge, the effect of method is obvious, but it grows the hardware cost of converter. Aiming at this, the paper provides a method, in which the voltage can be controlled; simultaneously the total harmonic distortion of input current will be reduced. The plan is expressed as follows.

Figure 12 shows the space vector modulation of TLC, which also includes four design criteria:

1. Every transfer should involve only on switch, one turned off or turned on, from one switching state to another;
2. Every cross should consider the minimum switching dissipation; in other word reduce the number of switching;
3. The switching sequence must consider the distributing of harmonic for the output voltage of TLC.
4. For the purpose of maintaining the switch state between each sector border, designed some boundary conditions in sector switch.

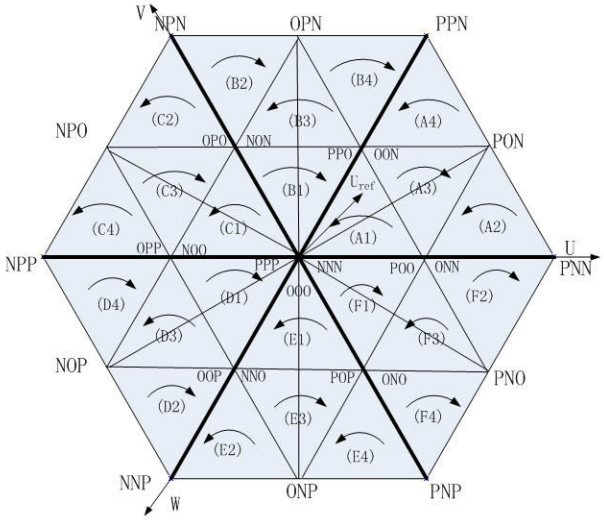

Fig.12 The space vector diagram of TLC

From figure 12 and principles, the vector sequence have special requirement, the switch count is limited, the switching loss is reduced, and the wave of input current is improved, but some time a part of conditions are contradictory.

In order to express the control strategy clearly, table 2 gives an example, assuming the reference voltage vector is falling into A1 region, and the strategy uses seven segment switching sequence.

Where P stands for the switch function S_{ip}=1; O stands for the switch function S_{im}=1; N stands for the switch function S_{in}=1; and the letter i will be a, b, or c phase. T_0, T_1, T_2 is the functionary time of switch sequence, which is computed by timing, and the concrete formula referenced the paper [15].

Table 2 Example of switching sequence

Scheme 1: clockwise			Scheme 2: clockwise		
Seg	Seq	Time	Seg	Seq	Time
1	ONN	$T_1/2+\triangle/2$	1	OON	$T_2/2+\triangle/2$
2	OON	$T_2/2$	2	OOO	$T_0/2$
3	OOO	$T_0/2$	3	POO	$T_1/2$
4	POO	$T_1/2-\triangle$	4	PPO	$T_2/2-\triangle$
5	OOO	$T_0/2$	5	POO	$T_1/2$
6	OON	$T_2/2$	6	OOO	$T_0/2$
7	ONN	$T_1/2+\triangle/2$	7	OON	$T_2/2+\triangle/2$

From table 2, the functionary time of switch contains a factor $\triangle$, it is a vector, which includes direction and magnitude, the direction will be built by the direction of phase current, and the magnitude will be decided by the range of neutral point potential. The detailed design principle is shown as follows.

Supposing to flow out the neutral point of current is the positive direction. Table 3 gives the relations between the voltage vector and the direction of phase current.

Table 3 The relationship between voltage vector and the direction of phase current

Vector	i_m	Vector	i_m	Vector	i_m
ONN	i_a	POO	$-i_a$	OPN	i_a
PPO	i_c	OON	$-i_c$	PON	i_b
NON	i_b	OPO	$-i_b$	NPO	i_c
OPP	i_a	NOO	$-i_a$	ONP	i_a
NNO	i_c	OOP	$-i_c$	NOP	i_b
POP	i_b	ONO	$-i_b$	PNO	i_c

Assuming to be the A1 region for the voltage vector, table 4 shows the mapping relation between neutral point voltage and phase current, from table 4, we can choose the direction of parameter $\triangle$. Similarly, if the voltage vector is in another region, we should choose the direction of parameter in according with phase current i_a i_b and i_c.

Table 4 The mapping relation between neutral point voltage and phase current

Neutral Point	i_m	i_a vs i_c	Direction i_a or i_c	$\triangle$
$U_{dc1}<U_{dc2}$	$i_m>0$	$\|i_a\|>\|i_c\|$	$i_a>0$	$\triangle>0$
			$i_a<0$	$\triangle<0$
		$\|i_a\|<\|i_c\|$	$i_c>0$	$\triangle<0$
			$i_c<0$	$\triangle>0$
$U_{dc1}>U_{dc2}$	$i_m<0$	$\|i_a\|>\|i_c\|$	$i_a>0$	$\triangle<0$
			$i_a<0$	$\triangle>0$
		$\|i_a\|<\|i_c\|$	$i_c>0$	$\triangle>0$
			$i_c<0$	$\triangle<0$

To refer table 2, table 3, table 4 and figure 12, we can decide the direction of parameter $\triangle$, but the magnitude of $\triangle$ didn't discuss, figure 13 showed the method, which will express the mathematic relation, and the parameter $\triangle$ is a ramp function.

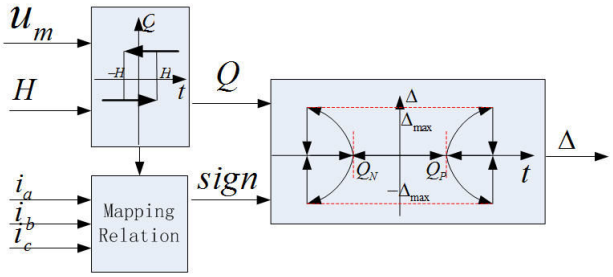

Fig.13 The diagram of control strategy

From figure 13, the parameter u_m is the neutral point voltage; 2H is the hysteresis bandwidth; Q is the enable signal; sign is the direction of $\triangle$, and the output signal is used to control voltage vector by mapping relation within table 2.

Certainly, in order to maintain the switch state around the sector border, this paper proposed boundary conditions. Figure 14 showed the fundamental principle, when the voltage vector is in the A1 region. If the border bandwidth is $2\triangledown$, table 5 gave the boundary expression.

Figure 15 showed an example for the implementation process of driver. The vector of A1 region is related with phase current i_a, $-i_a$ and $-i_c$, the current $-i_c$ can't restrain the voltage of neutral point, because of the current unidirectivity. On the contrary, it will affect the balance of neutral point; the i_a is the only adjusted factor, and the size of which is decided by the unbalanced degree of the neutral point potential. Certainly, in other regions, the i_b and i_c are the same function. In figure 14 if $u_m>0$, and $i_a>0$, the Δ must be more than zero, in other word, the functionary time of vector ONN will be lengthen, and the functionary time of vector POO will be shorten. At last, the normalized functionary time will be delivered to the compared register CMPRx of Digital Signal Processor (DSP).

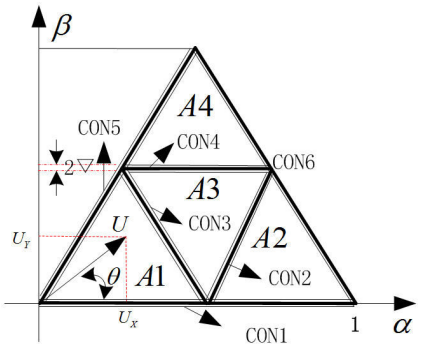

Fig.14 The fundamental principle of border

Table 5 The boundary conditions

Sector	Conditions
A1	$M \le \frac{\sqrt{3}/2 \pm \nabla}{\sin\theta + \sqrt{3}\cos\theta}$ $0 < \theta \le 60^\circ$
A2	$M > \frac{\sqrt{3}/2 \pm \nabla}{\sqrt{3}\cos\theta - \sin\theta}$ $M \le \frac{\sqrt{3} \pm \nabla}{\sqrt{3}\cos\theta + \sin\theta}$ $\theta < 30^\circ$
A3	$M > \frac{\sqrt{3}/2 \pm \nabla}{\sin\theta + \sqrt{3}\cos\theta}$ $M \le \frac{\sqrt{3}/2 \pm \nabla}{\sqrt{3}\cos\theta - \sin\theta}$ $\theta < 30^\circ$ $M \le \frac{\sqrt{3}/4 \pm \nabla}{\sin\theta}$ $30^\circ < \theta < 60^\circ$
A4	$M > \frac{\sqrt{3}/4 \pm \nabla}{\sin\theta}$ $30^\circ < \theta < 60^\circ$

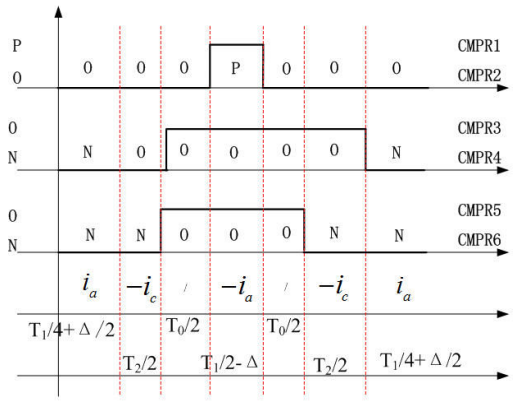

Fig.15 The implementation process of driver

In a word, the potential of neutral point is in connection with the current of neutral point, which is inflow or outflow. The control strategies will improve the stability of neutral point voltage largely, and don't increase cost of hardware. In high power field, the strategy will be used widely.

5 Simulation Results

A detail mathematical model of PET was analyzed, and the controllers were developed in the MATLAB/SIMULINK environment. Based on the parameters in table 6, some simulation results were shown in the following statement.

Assuming to the balanced power system, The following cases have been studied, in order to verify the new topology of PET, figure 16 (a) (b) showed the waves of DC-bus voltage in steady state, as a result of that, the DC-bus voltage is homeostatic under proposed control strategies, even small interferential signal existed, but the voltage of DC-bus includes triple frequency of fundamental wave, and the fluctuation of voltage is less than $20V_{pp}$. Figure 17 (a) showed the waves of neutral point voltage, and proved that the control strategies of neutral point voltage are feasible.

Table 6 System parameter for simulation

PARAMETER	VALUE
Rated power	50kVA
Grid voltage	10kV
Line frequency	50Hz
Carrier frequency	8kHz
Output inductance	700uH
Output capacitor	100uF×2
Damping resister	0.5Ω
DC-Bus capacitor	5mF
Rated DC voltage	800V

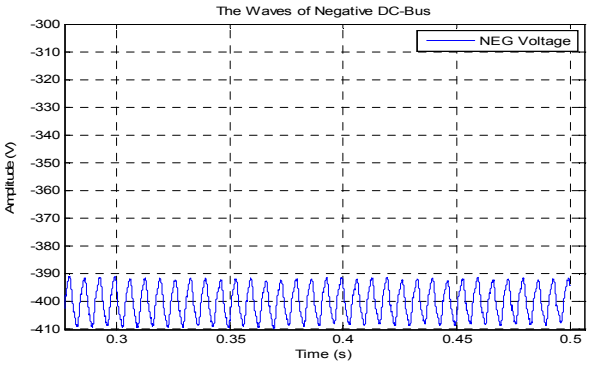

(a) Voltage of negative DC-Bus

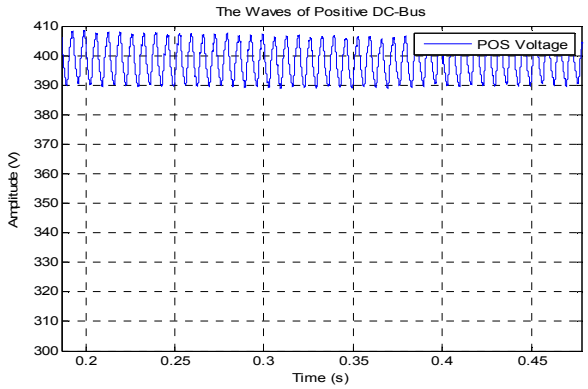

(b) Voltage of positive DC-Bus

Fig.16 The DC-Bus voltage in steady state

From figure 17 (b), if without neutral point control strategy, DC bus voltage will be unbalanced. Normally the system will be unstable, and the total harmonic distortion of input or output waves will be higher.

At the same time, because of the adjusted control, the DC bus can be used to integrate distributed power, such as renewable energy source.

In Smart-Grid era, it is a possible to establish DC distributed network, and PET will be used to manage power flow.

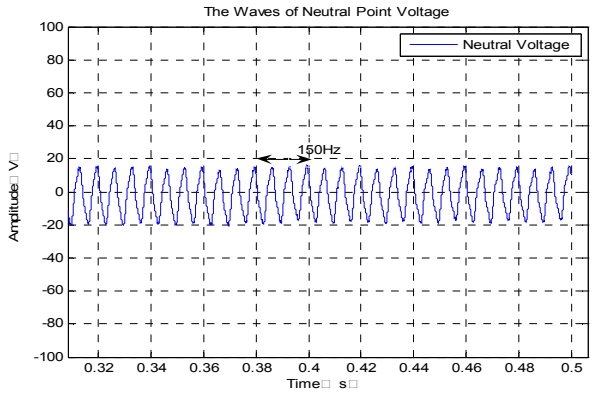

(a) The neutral point voltage with control strategy

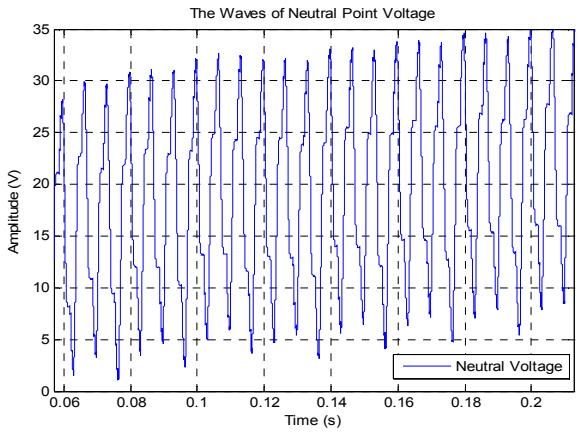

(b) The neutral point voltage without control strategy

Fig.17 The waves of neutral point voltage

Figure 18 showed the output line voltage of PET in steady state, and figure 19 expressed the voltage spectrum analysis chart, which indicated that the output voltage of PET is smooth. If DC-Bus had been connected storage devices, whenever and whatever the power system is, the output waves of PET will be constant. In addition, the harmonic of system didn't affect the quality of output voltage. The nonlinear load didn't also influence power system, so PET realized the separated function like both traditional power transformer and DFACTs.

Figure 20 (a) (b) showed the waves of output voltage and current, when the load is in step response from 24kVA to 48kVA, and from 48kVA to 24kVA. Additionally, the power factor is 0.7. It can be seen that the performance of converter based on voltage source is great, which can be adjusted with variable load.

From the simulation results, the control strategies of PET are valid, in which the neutral point voltage and the output voltage are controlled smoothly, and the new topology of PET is valid.

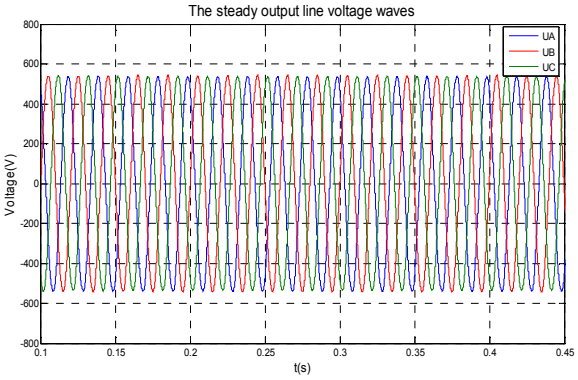

Fig.18 The steady state waves of output voltage

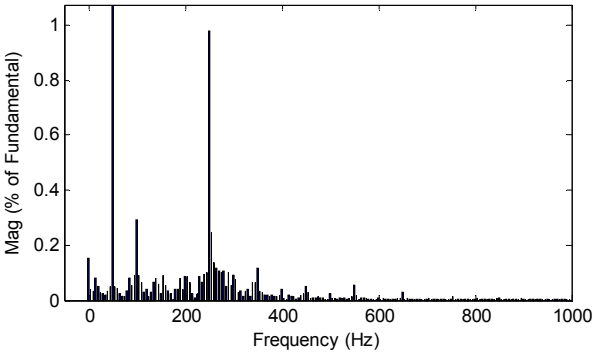

Fig.19 The voltage spectrum analysis chart

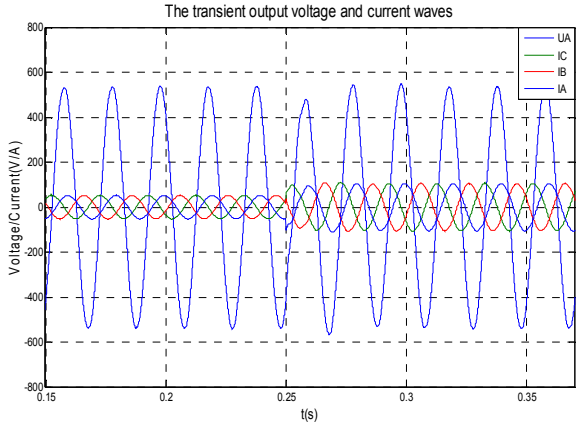

(a) The step response from 24kVA to 48kVA

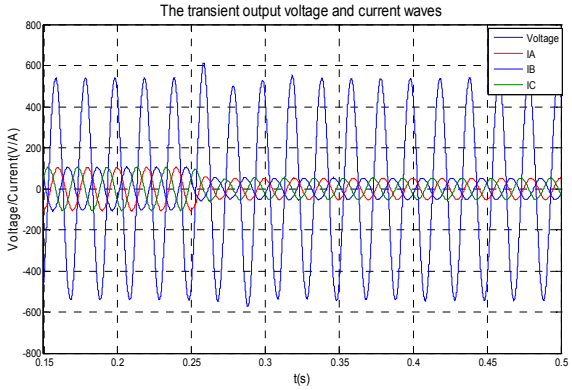

(b) The step response from 48kVA to 24kVA

Fig.20 The waves of output voltage and current

6 Experimental results

A prototype 40kVA PET for a simple power distribution system has been implemented with IGBT module at laboratory. Table 7 showed the parameters of PET.

In order to verify the strategies of neutral point voltage, and proof the control performance, the next experimental results had been done. The stable DC bus voltage ripple was measured as shown in figure 21, and figure 21 (a) (b) gave the neutral point voltage, of which the CH2 is positive bus, the CH1 is negative bus, and the difference of CH1 and CH2 is neutral point voltage, from figures as we know, the voltage waves aren't smooth enough, because of the interference of high voltage probe, and other stray parameters.

Table 7 The parameters of PET prototype

PARAMETER	VALUE
Rated Power	40kVA
Grid Voltage	380V
Line Frequency	50Hz
Carrier Frequency	7.2kHz
Output Inductance	700uH
Output Capacitor	100uF×2
Damping Resistor	0.5Ω
DC-bus Capacitor	3.4mF
Rated DC voltage	800V

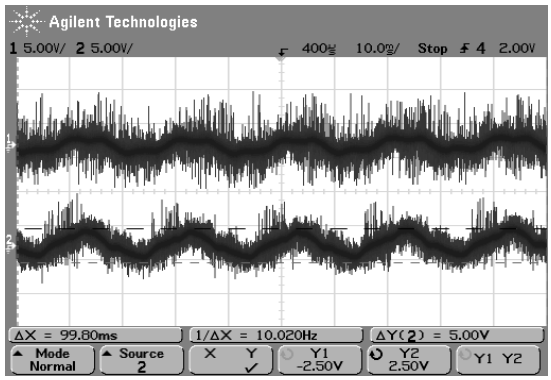

a) DC bus voltage

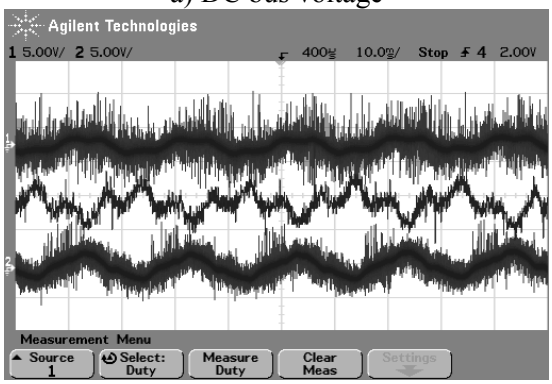

b) Neutral point voltage

Fig.21 the waves of voltage

Figure 22 showed the output voltage waves. Figure 22 (a) expressed stable voltage waves and neutral point voltage wave, it is obvious that the waves includes triple frequency of fundamental wave, and figure 22 (b) provided transient voltage waves, which located by shocking loads from 0kW to 10kW, and the deviation rate is less than 1.25%, the restoring time is zero. The CH1 is current, and the CH4 is voltage; figure 22 (c) gave the other wave, which showed by shocking loads from 10kW to 0kW, and the deviation rate is less than 0.597%, the restoring time is zero yet.

From above figures as we know, the experiments do consist with simulation results; the structure of PET is feasible.

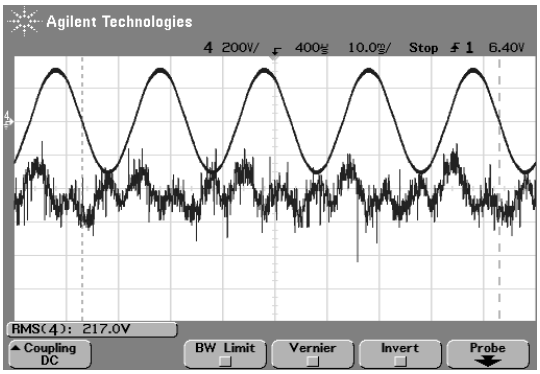

a) Stable voltage and Neutral point voltage

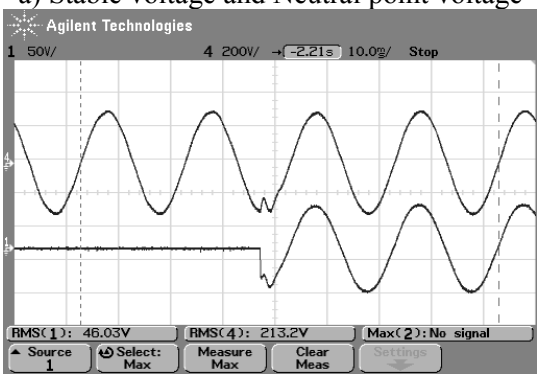

b) Transient response waves

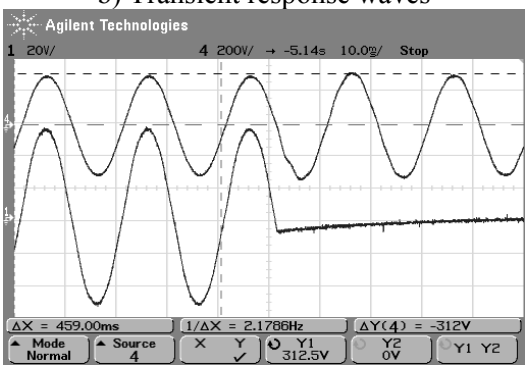

c) Transient response waves

Fig.22 The waves of voltage and current

7 Conclusion

This paper proposed a new topology of Power Electronic Transformer based on the development of power electronic device and the manufacturing level of high-frequency transformer, then analyzed the mathematical model of PET in detail, and indicated the fault of the topology, which is the unbalance of neutral point voltage.

At the same time, the paper proposed the reasons of causing unbalance of voltage, and supplied the solution based on SVM for this problem. In the meanwhile, the method has considered the distortion of output voltage, and the count of switching.

In conclusion, the simulation and experimental results verified the feasibility of the new topology. Therefore, PET will be speeded up the industrialization process.

References:

[1] Moonshik Kang, Prasad N. Enjeti, Ira J. Pitel, Analysis and Design of Electronic Transformers for Electric Power Distribution System, *in Proc. 1997 IEEE Industry Application Society Annual Meeting*, Vol.5, NO.11, 1997, pp. 1689-1694.

[2] H. Iman-Eini, S. Farhangi, Analysis and Design of Power Electronic Transformer for Medium Voltage Levels, *in Proc. 2006 IEEE Power Electronics Specialists Conference*, Vol.21, NO.9, 2006, pp. 1-5.

[3] Jin Ping, Guo Jianbo, Zhao Bo, Zhou Fei, Wang Zhibing, Applications of Power Electronics Technology in Strong&Smart Grid, *Power System Technology*, Vol.33, NO.15, 2009, pp. 1-7.

[4] Frank R.Goodman,Jr., The EPRI Intelligent Universal Transformer (IUT), *Workshop on International Standardization for Distributed Energy Resources*, Vol.8, NO.10, 2009, pp. 14-28.

[5] Manjrekar M D, Kieferndorf R, Venkataramanan G, Power Electronic Transformers for Utility Application, *In conference record of the 2000 IEEE Industry Application Conference*, Vol.12, NO.11, 2000, pp. 2496-2502.

[6] Edward R. Ronan, Scott D. Sudhoff, Steven F. Glover, Dudley L. Galloway. A Power Electronic Based Distribution Transformer, *IEEE Transactions on Power Delivery*, Vol.17, NO.14, 2002, pp. 1231-1238.

[7] Harada K, Anan F, Yamasaki K. Intelligent Transformer, *In Proceedings of the 1996 IEEE PESC*, Vol.4, NO.7, 1996, pp. 1337-1341.

[8] Holger Wrede, Volker Staudt, Andreas Steimel, Design of an electronic power transformer, *In: Proceedings of the 28 IEEE/IES Annual Conference*, 2002, pp. 1380-1385.

[9] Jae Hyeong Seo, Chang Ho Choi, Dong Seok Hyum, A new simplified space vector pwm method for three level inverters, *In Proceedings of IEEE Transactions on Power Electronics*, Vol.16, NO.5, 2001, pp. 1025-1032.

[10] Meng YongQing, Liu Zheng, Su YanMin, A novel SVM method for three-level pwm voltage source inverter, *In Proceedings of the 30th annual conference of the IEEE Industrial Electronics Society*, Vol.21, NO.23, 2004, pp. 321-328.

[11] C. K. Lee, S. Y.R.Hui, H. Shu-Hung, Yash Shrivastava, A randomized voltage vector switching scheme for three level power inverters, *In Proceedings of the IEEE Transactions on Power Electronics*, Vol.17, NO.3, 2002, pp. 1154-1162.

[12] Ramon C, MaAngeles Martin Prats, Modeling strategy for back-to-back three level converters applied to high power wind turbines, *In Proceedings of IEEE Transaction on Industrial Electronics*, Vol.53, NO.15, 2006, pp. 1331-1339.

[13] Juan Manuel Carrasco, Leopoldo Garcia Franquelo, Power Electronic Systems for the Grid Integration of Renewable Energy Sources: A Survey, *In Proceedings of IEEE Transaction on Industrial Electronics*, Vol.53, NO.2, 2006, pp. 1245-1254.

[14] Katuji Shinohara, Eiichi Sakasegawa, A new pwm method with suppressed neutral point potential variation of three-level inverter for AC servo motor drive, *In Proceedings of IEEE 1999 International Conference on Power Electronics and Drive System*, Vol.7, NO.5, 1999, pp. 981-989.

[15] R.S. Kanchan, M.R. Baiju, K.K. Mohapatra, P.P. Ouseph, K. Gopakumar, Space vector pwm signal generation for multilevel inverters using only the sampled amplitudes of reference phase voltages, *In Proceeding of IEE Proc-Electr. Power Appl*, Vol.152, NO.2, 2005, pp. 1131-1139.

[16] M. R. Banaei, E. Salary, Mitigation of Current Harmonics and Unbalances Using Power Electronic Transformer, In 25th International Power System Conference, Vol.10, NO.1, 2010, pp. 1-9.